First-principles calculation of excited states of diatomic molecules: A benchmark for the Gutzwiller conjugate gradient minimization method

Zhuo Ye,[1,] Yong-Xin Yao,[1] Cai-Zhuang Wang,[1] Kai-Ming Ho[1,2*]*

[1] Ames Laboratory – US DOE and Department of Physics and Astronomy, Iowa State University, Ames, Iowa 50011, United States

[2] Hefei National Laboratory for Physical Sciences at Microscale, International Center for Quantum Design of Functional Materials (ICQD) and Synergetic Innovation Center of Quantum Information and Quantum Physics, University of Science and Technology of China, Hefei, Anhui 230026, China

Keywords: correlated electron systems, Gutzwiller wave function, excited states, potential energy curve

* E-mail: zye@iastate.edu (Z.Y.) kmh@iastate.edu (K.M.H.)

ABSTRACT

We recently proposed the Gutzwiller conjugate gradient minimization (GCGM) method for efficient and accurate calculation of the ground state total energy of molecular and bulk systems. The GCGM method is developed under the framework of Gutzwiller wave function but goes beyond the commonly adopted Gutzwiller approximation to improve the accuracy and flexibility in treating the correlation effects. In this conference proceeding, we benchmark the GCGM method with calculation of excited state potential energy curves of 3 diatomic molecules, namely, H_2, N_2, and O_2. Our calculations demonstrate the flexibility and reasonable accuracy of the method.

1. INTRODUCTION

One of the most fundamental challenges in physics, chemistry and materials science is accurate and efficient ab initio calculation of correlated electron systems. Understanding and controlling the properties of matter that emerge from their complex correlations of atomic or electronic constituents calls for accurate theoretical methods to describe correlation effects. At the same time, it is often highly desirable that the methods are compuationally efficient, especially for large systems. In many cases, a trade-off between accuracy and speed has to be made as it is rather challenging to find a method that can achieve both. Various theoretical approaches have been proposed with respect to specific speed-accuracy trade-off for different target systems. On one end, considerations of speed are neglected to achieve the highest possible accuracy while on the other end, accuracy is sacrificed for a favorable speed. These two ends span a whole spectrum of different approaches, ranging from very fast but inaccurate to very accurate but slow. The density functional theory (DFT) [1,2] is very fast and has been very successful in predicting the structures and properties of many materials. However, a great challenge of DFT is that comparatively simple density functional approximations are not sufficiently accurate to describe strongly-correlated electron materials. On the other end of the spectrum are, for example, some wave function-based quantum chemistry methods, especially the multi-configurational self-consistent field (MCSCF) approaches [3], such as complete active space SCF (CASSCF) [4] and the restricted active space SCF (RASSCF) [5,6]. They can be very accurate, but require a heavy workload even after the efficiency has been promoted by using the density-

matrix renormalization group (DMRG) [7-9]. Quantum Monte Carlo (QMC) methods [10-12] can also be very accurate as demonstrated by studies of realistic correlated-electron materials, but still, they are computationally expensive. In the middle of the spectrum are, for example, some hybrid approaches that combine DFT and many-body techniques, such as DFT+onsite Coulomb interaction (DFT+U) [13,14], DFT+dynamical mean-field theory (DMFT) [15,16], and DFT+Gutzwiller [17-20]. Besides accuracy and efficiency, being universal and flexible is another desirable characteristic of the methods to describe correlation effects. Some methods, for example, the aforementioned hybrid approaches that combine DFT and many-body techniques, have been demonstrated to be very effective in describing the properties of real correlated-electron materials. However, the predictive power of these method is limited by the use of adjustable screened Coulomb parameters.

Gutzwiller wavefunctions (GWF) have been widely used for computationally efficient description of strongly correlated systems [17,21-24]. Although methods based on the GWF are fast, often they are insufficiently accurate. Recently, we have been working on improving the accuracy and developed two approaches, the correlation matrix renormalization (CMR) method [25-28] and later the Gutzwiller conjugate gradient minimization (GCGM) method [29], for computationally efficient calculation of the ground state total energy of molecular and bulk systems. Both approaches minimize the energy of a system which is described with a GWF constructed by applying a correlation operator on a trial noninteracting wavefunction such that each on-site valence electronic configuration obtains an appropriate amplitude and phase

factor. The CMR method adopts the Gutzwiller variational wave functions and uses the Gutzwiller approximation (GA) and Hartree-Fock (HF) type factorization to treat the intersite Coulomb interactions, thus greatly enhances the computational efficiency. As illustrated in Ref. [27], the resulting errors from the use of Wick's theorem have been greatly reduced by implementing the sum-rule correction, and the CMR method can achieve a reasonable accuracy for correlated-electron systems with compuational effort scaling as N^4 with respect to the system size N, like HF. Nevertherless, the use of the GA, i.e. the inter-site decoupling approximation, may still be a major source of inaccuracy. The GCGM method was then developed to go beyond the intersite decoupling approximation to obtain more accurate result. Another advantage of GCGM is that it does not require the trial wavefunction on which the GWF is constructed to be a single Slater determinant, thus adds more freedom for the trial wavefunction. As shown in Ref. [29], the GCGM method yields resonably accurate ground state total energies of molecular and bulk systems.

Methods in the Gutzwiller framework work well for describing the ground state, which is also true for many other methods based on the variational principle. The question remains, however, as to whether these methods can be extended to describe excited states. The CMR method, for example, cannot be straightforwardly generalized for excited states. In this conference proceeding, we demonstrate the power of the GCGM method for describing excited states by presenting benchmark results of 3 diatomic systems, namely, H_2, N_2, and O_2, in comparison with large-basis CI calculations and expermimental observations. Our calculations illustrate the flexibility

and reasonable accuracy of the method.

2. METHODS

In the form of second quantization, the full ab initio nonrelativistic Hamiltonian for an interacting many-electron system can be expressed as,

$$H = \sum_{i\alpha j\beta,\sigma} t_{i\alpha j\beta} c^{\dagger}_{i\alpha\sigma} c_{j\beta\sigma} + \frac{1}{2} \sum_{\substack{i\alpha j\beta \\ k\gamma l\delta,\sigma\sigma'}} u(i\alpha j\beta;k\gamma l\delta) c^{\dagger}_{i\alpha\sigma} c^{\dagger}_{j\beta\sigma'} c_{l\delta\sigma'} c_{k\gamma\sigma}, \quad (1)$$

where $c^{\dagger}_{i\alpha\sigma}$ ($c_{i\alpha\sigma}$) is the creation (annihilation) operator which creates (annihilates) an electron of spin σ in orbital α at site i. i, j, k, l are the atomic site indices, $\alpha, \beta, \gamma, \delta$ the site-centered orbital indices, and σ, σ' the spin indices. Here, t and u are the one-electron hopping integral and the two-electron Coulomb integral, respectively, and are defined in Eq. (2) and (3),

$$t_{i\alpha j\beta} = \left\langle \phi_{i\alpha} \left| \hat{T} + \hat{V}_{ion} \right| \phi_{j\beta} \right\rangle, \quad (2)$$

$$u(i\alpha j\beta;k\gamma l\delta) = \iint d\mathbf{r} d\mathbf{r}' \phi^{*}_{i\alpha}(\mathbf{r}) \phi^{*}_{j\beta}(\mathbf{r}') \hat{U}(\mathbf{r}-\mathbf{r}') \phi_{l\delta}(\mathbf{r}') \phi_{k\gamma}(\mathbf{r}), \quad (3)$$

where $\hat{T}$, $\hat{V}_{ion}$, and $\hat{U}$ are the operators for kinetic energy, ion-electron interaction and Coulomb interaction, respectively. $\phi_{i\alpha}$ is the α^{th} orbital at the i^{th} site.

As shown in Eq. (1), all interactions are included in the Hamiltonian without any adjustable parameters. In our GCGM approach, the total energy is evaluated with the GWF of the form,

$$\left|\Psi_{GWF}\right\rangle = \sum_{\{\Gamma_i\}}\left(\prod_i g(\Gamma_i)\right)\left|\{\Gamma_i\}\right\rangle\left\langle\{\Gamma_i\}\right|\left.\Psi_0\right\rangle, \tag{4}$$

which is constructed based on the trial wave function $\left|\Psi_0\right\rangle$. In this work, we use a restricted Hartree-Fock (RHF) wave function as $\left|\Psi_0\right\rangle$ unless stated otherwise. The occupation of molecular orbitals in $\left|\Psi_0\right\rangle$ can be changed to get the corresponding excited states. However, we would like to note that $\left|\Psi_0\right\rangle$ does not have to be non-interacting or a single Slater determinant. $g(\Gamma_i)$ is the Gutzwiller variational parameter determining the occupation probability of the on-site configuration $\left|\Gamma_i\right\rangle$, which is defined as a Fock state at the i^{th} site $\left|\Gamma_i\right\rangle \equiv \prod_{\alpha\sigma\in\Gamma_i} c_{\alpha\sigma}^{\dagger}\left|\varnothing\right\rangle$. $\left|\varnothing\right\rangle$ is the Fermionic vacuum that contains no electrons. The total energy can be expressed as,

$$E_{GWF} = \sum_{i\alpha j\beta,\sigma} t_{i\alpha j\beta}\left\langle c_{i\alpha\sigma}^{\dagger}c_{j\beta\sigma}\right\rangle_{GWF} + \frac{1}{2}\sum_{\substack{\text{ijkl},\alpha\beta\gamma\delta \\ \sigma\sigma'}} u(i\alpha j\beta;k\gamma l\delta)\left\langle c_{i\alpha\sigma}^{\dagger}c_{j\beta\sigma'}^{\dagger}c_{l\delta\sigma'}c_{k\gamma\sigma}\right\rangle_{GWF} \tag{5}$$

Here, for any operator $\hat{O}$, $\left\langle\hat{O}\right\rangle_{GWF}$ is a short-hand notation for $\left\langle\Psi_{GWF}\left|\hat{O}\right|\Psi_{GWF}\right\rangle$. We treat the on-site two particle correlation matrix (2PCM, or equivalently the two-body reduced density matrix) rigorously and evaluate the inter-site 2PCM using the Hartree-Fock(HF)-type factorized approximation (Wick's theorem, see Ref. [27,30]),

$$\begin{aligned}&\left\langle c_{i\alpha\sigma}^{\dagger}c_{j\beta\sigma'}^{\dagger}c_{l\delta\sigma'}c_{k\gamma\sigma}\right\rangle_{GWF} \approx \\ &\quad\left\langle c_{i\alpha\sigma}^{\dagger}c_{k\gamma\sigma}\right\rangle_{GWF}\left\langle c_{j\beta\sigma'}^{\dagger}c_{l\delta\sigma'}\right\rangle_{GWF} - \delta_{\sigma\sigma'}\left\langle c_{i\alpha\sigma}^{\dagger}c_{l\delta\sigma}\right\rangle_{GWF}\left\langle c_{j\beta\sigma}^{\dagger}c_{k\gamma\sigma}\right\rangle_{GWF}\end{aligned} \tag{6}$$

After using the approximation in Eq. (6) for inter-site 2PCM, Eq. (5) becomes,

$$E_{GWF} = \sum_{i\alpha j\beta,\sigma} t_{i\alpha j\beta} \left\langle c^{\dagger}_{i\alpha\sigma} c_{j\beta\sigma} \right\rangle_{GWF} + \frac{1}{2} \sum_{\substack{i,\alpha\beta\gamma\delta \\ \sigma\sigma'}} u(i\alpha i\beta; i\gamma i\delta) \left\langle c^{\dagger}_{i\alpha\sigma} c^{\dagger}_{i\beta\sigma'} c_{i\delta\sigma'} c_{i\gamma\sigma} \right\rangle_{GWF}$$
$$+ \frac{1}{2} \sum_{\substack{i\alpha j\beta \\ k\gamma l\delta,\sigma\sigma'}}{}' \left(u(i\alpha j\beta; k\gamma l\delta) - \delta_{\sigma\sigma'} u(i\alpha j\beta; l\delta k\gamma) \right) \left\langle c^{\dagger}_{i\alpha\sigma} c_{k\gamma\sigma} \right\rangle_{GWF} \left\langle c^{\dagger}_{j\beta\sigma'} c_{l\delta\sigma'} \right\rangle_{GWF} \tag{7}$$

where $\sum'$ indicates that the pure on-site terms are excluded from the summation. The HF-type approximation in Eq. (6) will introduce errors. However, as Ref. [27] shows, the sum-rule correction can efficiently reduce this factorization error by shifting the non-local intersite terms to local onsite terms, which can be evaluated more accurately. So the sum-rule correction is inherited here in the GCGM method for the same purpose. When we evaluate the energy, we include the sum-rule part H_{sr} in Eq. (8) in the Hamiltonian H in Eq. (1),

$$H_{sr} = \frac{1}{2} \sum_{i\alpha} \lambda_{i\alpha} \left(\hat{n}_{i\alpha\sigma} \left(\sum_{j\beta\sigma'} \hat{n}_{j\beta\sigma'} - N_e \right) \right) \tag{8}$$

Here $\lambda_{i\alpha}$ is determined by the weighted average of the relevant inter-site 2-electron Coulomb integrals,[1]

$$\lambda_{i\alpha} = -\frac{\sum_{j\neq i,\beta\sigma'} u(i\alpha j\beta; i\alpha j\beta) R_{ij}^{-6}}{\sum_{j\neq i,\beta\sigma'} R_{ij}^{-6}}, \tag{9}$$

where R_{ij} is the distance from atom i to atom j.

We consider a dimer that has only 2 sites. The one-particle density matrix (1PDM) can be expressed as,

[1] The specific form in Eq. (9) is not unique. It works as long as the weight decreases sufficiently fast with respect to the inter-atomic separations. In other words, the dominant contribution comes from the nearest neighbors.

$$\left\langle c_{i\alpha\sigma}^{\dagger} c_{i\beta\sigma} \right\rangle_{GWF} = \frac{1}{\left\langle \Psi_{GWF} \middle| \Psi_{GWF} \right\rangle} \sum_{\Gamma_i, \Gamma'_i, \Gamma_j} \left\langle \Gamma_i \middle| c_{i\alpha\sigma}^{\dagger} c_{i\beta\sigma} \middle| \Gamma'_i \right\rangle g(\Gamma_i) g(\Gamma'_i) g(\Gamma_j)^2 \xi^0_{\Gamma_i, \Gamma_j, \Gamma'_i, \Gamma_j} \tag{10}$$

$$\left\langle c_{i\alpha\sigma}^{\dagger} c_{j\beta\sigma} \right\rangle_{GWF} = \frac{1}{\left\langle \Psi_{GWF} \middle| \Psi_{GWF} \right\rangle} \sum_{\Gamma_i, \Gamma_j, \Gamma'_i, \Gamma'_j} \left\langle \Gamma_i \middle| c_{i\alpha\sigma}^{\dagger} \middle| \Gamma'_i \right\rangle \left\langle \Gamma_j \middle| c_{j\beta\sigma} \middle| \Gamma'_j \right\rangle \cdot g(\Gamma_i) g(\Gamma_j) g(\Gamma'_i) g(\Gamma'_j) \xi^0_{\Gamma_i, \Gamma_j, \Gamma'_i, \Gamma_j} \quad \textit{for } i \neq j \tag{11}$$

where $\xi^0_{\Gamma_i, \Gamma_j, \Gamma'_i, \Gamma_j}$ is predetermined coefficient from $\left| \Psi_0 \right\rangle$,

$$\xi^0_{\Gamma_i, \Gamma_j, \Gamma'_i, \Gamma_j} = \left\langle \Psi_0 \middle| \Gamma_i, \Gamma_j \right\rangle \left\langle \Gamma'_i, \Gamma'_j \middle| \Psi_0 \right\rangle \tag{12}$$

and $\left\langle \Psi_{GWF} \middle| \Psi_{GWF} \right\rangle = \sum_{\Gamma_i, \Gamma_j} \xi^0_{\Gamma_i, \Gamma_j, \Gamma'_i, \Gamma_j} g(\Gamma_i)^2 g(\Gamma_j)^2$ (13)

The on-site 2PCM $\left\langle c_{i\alpha\sigma}^{\dagger} c_{i\beta\sigma}^{\dagger}, c_{i\gamma\sigma}, c_{i\delta\sigma} \right\rangle_{GWF}$ can be expressed as,

$$\left\langle c_{i\alpha\sigma}^{\dagger} c_{i\beta\sigma}^{\dagger}, c_{i\nu\sigma}, c_{i\delta\sigma} \right\rangle_{GWF} = \frac{1}{\left\langle \Psi_{GWF} \middle| \Psi_{GWF} \right\rangle} \sum_{\Gamma_i, \Gamma'_i, \Gamma_j} \left\langle \Gamma_i \middle| c_{i\alpha\sigma}^{\dagger} c_{i\beta\sigma}^{\dagger}, c_{i\nu\sigma}, c_{i\delta\sigma} \middle| \Gamma'_i \right\rangle g(\Gamma_i) g(\Gamma'_i) g(\Gamma_j)^2 \xi^0_{\Gamma_i, \Gamma_j, \Gamma'_i, \Gamma_j} \tag{14}$$

We note that the expressions in Eq. (10)(11)(14) are rigorous. In the GA, an element of one-particle density matrix expressed in the $\left| \Psi_{GWF} \right\rangle$ can be approximated by the multiplication of the corresponding element in the $\left| \Psi_0 \right\rangle$ and the one-electron renormalization z-factor that is assigned to each of the two relevant sites, i.e. $\left\langle c_{i\alpha\sigma}^{\dagger} c_{j\beta\sigma} \right\rangle_{GWF} \approx z_{i\alpha\sigma} z_{j\beta\sigma} \left\langle c_{i\alpha\sigma}^{\dagger} c_{j\beta\sigma} \right\rangle_0$, where the z-factor is a function of the Fock states occupation probabilities. Here $\left\langle c_{i\alpha\sigma}^{\dagger} c_{j\beta\sigma} \right\rangle_0$ is a short-hand notation for $\left\langle \Psi_0 \middle| c_{i\alpha\sigma}^{\dagger} c_{j\beta\sigma} \middle| \Psi_0 \right\rangle$. One can see that the GA "decouples" the two correlated sites by using a site-site factorization and this inter-site decoupling approximation is a major source of inaccuracy. Our method goes beyond the GA by rigorously evaluating the

1PDM and thus improves the accuracy.

With the 1PDM and the 2PCM evaluated, E_{GWF} can be expressed explicitly as a function of $\{g(\Gamma_i)\}$. E_{GWF} is then minimized with respect to $\{g(\Gamma_i)\}$ with the conjugate gradient method after the derivatives $\frac{\partial E_{GWF}}{\partial g(\Gamma_i)}$ are evaluated. We note that the major computational burden of GCGM, the evaluation of the derivatives $\frac{\partial E_{GWF}}{\partial g(\Gamma_i)}$, can be readily partitioned with regard to the configuration Γ_i, as the evaluation of an individual derivative is independent of other derivatives. Therefore, the computational workload of the approach can be easily handled by efficient parallel computing.

The extension of GCGM method to molecules with more than 2 atoms or bulk materials is straightforward and is described in Ref. [29]. We will not present the formalism for bulk systems here, since we will focus on diatomic systems only and benchmark our GCGM method with energy calculations of excited states of both spin-unpolarized and spin-polarized systems. Nevertheless, it is worth noting that the GCGM is characterized with a good scaling with system size and makes possible fast and accurate calculations of large molecules or bulk systems. It is quasi-linearly scaled with the number of pairs of atoms to be considered in the system, i.e. $N-1$ for periodic bulk systems or $N(N-1)/2$ for molecules with N atoms [29].

3. RESULTS AND DISCUSSIONS

To demonstrate the effectiveness of the method, we show the GCGM energies for the ground and first few excited states of 3 diatomic systems, H_2, N_2, and O_2. For H_2 and N_2, the ground state is spin-singlet while for O_2, the ground states are spin-triplets. Although it is often staightforward to work with minimal basis-set orbitals, accurate calculations that can be compared with experiments call for the utilization of converged large basis-set orbitals. However, the use of large basis-set orbitals will greatly increase the computational complexity. To address this issue, we take advantage of QUAsi-atomic Minimal Basis set Orbitals (QUAMBOs), which have been illustrated to be good approximations to the multi-configurational self-consistent field (SCF) determined correlating orbitals [31]. In addition to occupied SCF orbitals, QUAMBOs also contain information about the virtural valence orbitals, thus can recover most of the static correlation energy. In this work, QUAMBOs are constructed based on large-basis HF calculations with the aug-cc-pVTZ basis functions [32]. QUAMBOs are used with the $1s$ for H_2, $2s$ and $2p$ orbitals for N_2 and O_2, chosen as the on-site correlated orbitals. After QUAMBOs are constructed as basis-set orbitals, the restricted Hartree-Fock (RHF) wave function is used as $|\Psi_0\rangle$ unless stated otherwise. The occupation of molecular orbitals in $|\Psi_0\rangle$ can be changed to get the corresponding excited states. The steps to predict (low energy) excited states within the GCGM method are well defined. It starts with the construction of a new single-Slater determinant $|\Psi_0\rangle$ with electrons excited from occupied molecular orbitals to unoccupied orbitals, e.g., single excitation or double excitation. A new Gutzwiller wave function can be constructed by applying correlation projector on the new $|\Psi_0\rangle$. It is subsequently optimized within the GCGM

approach and an excited state is obtained. A list of low energy excited states can thus be calculated by repeating the above procedure. QUAMBO-based FCI, large-basis CI results and experimental measurements are also presented for comparison. To compare with large-basis CI and experiment, dynamical correlation beyond the minimal basis calculations needs to be included. For simplicity, we adopt the local density approximation (LDA) for the dynamical correlation energy E_c and evaluate it with the PySCF package [33].

3.1. H_2

We focus on energy calculations of the states with atomic limits being $H(^1S)+H(^1S)$. There are 4 states with this atomic limit. The ground state $^1\Sigma_g^+$ is a singlet and the 3 degenerate excited states $^3\Sigma_u^+$ are triplets. Fig. 1(a) plots the potential energy curve evaluated by GCGM and QUAMBO-based FCI. The occupancies of molecular orbitals in the intial trial wave function are changed accordingly to calculate the excited states. The GCGM method produces energies in good agreement with FCI with minimum basis. The potential energy curve measured by experiment for the ground state is also plotted for comparison. For the ground state $^1\Sigma_g^+$, the discrepancy between QUAMBO-CI and experiment of the binding energy is not big, ~0.01 Hartree. For the excited triplet states, however, the discrepancy at $r < 1\text{Å}$ is noticeable, indicating that the minimum basis may not be enough to describe the excited dimer at short bond length. Fig. 1(b) plots the GCGM $+E_c$ results in comparison with experiment [34]. GCGM $+E_c$ yields energies in slightly better agreement with

experiment than GCGM does. Discrepancies still exist though, as it is a challenging problem to recover all of the dynamical correlation beyond the minimal basis calculations. It is not surprising that inclusion of E_c has limited impact on the total energy, as a weak correlation energy is expected for a system like H_2.

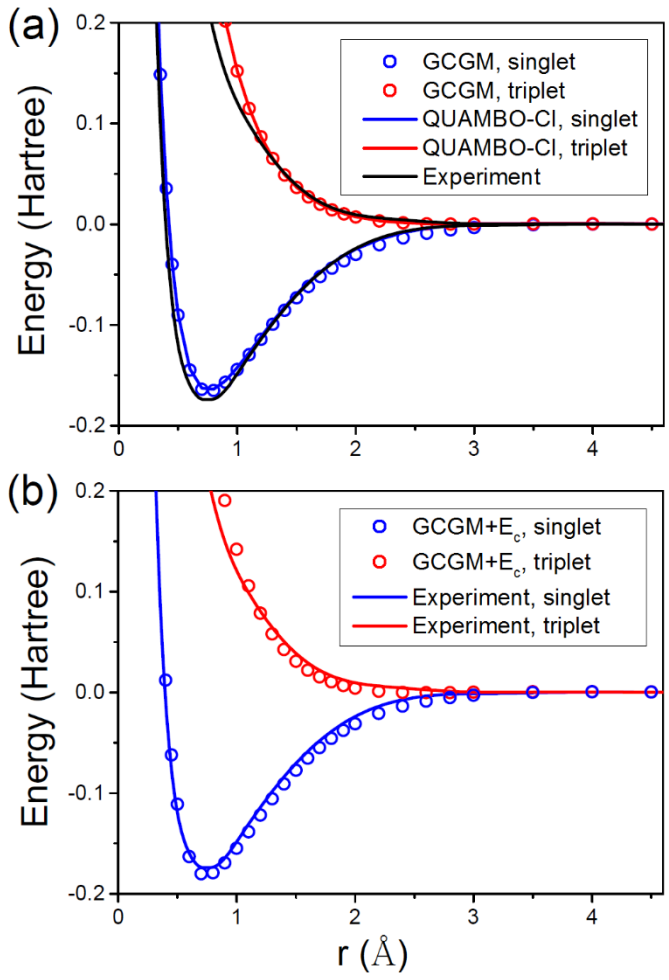

Figure 1. Potential energy curves of H_2 determined by (a) GCGM, QUAMBO-CI and experiment [34], and (b) GCGM+E_c and experiment. The GCGM and QUAMBO-CI calculations are based on QUAMBOs constructed from the aug-cc-pVTZ basis set.

3.2. N_2

N_2 has served as a benchmarking system with several theoretical methods [35]. Here, we focus on energy calculations of the states with atomic limits being $N(^4S^0)+N(^4S^0)$. There are 11 states with this atomic limit, of which the ground singlet state $^1\Sigma_g^+$ and the 1st excited triplet states $A^3\Sigma_u^+$ are bound, and the next excited septet states $^7\Sigma_u^+$ are unbound. For simplicity, we only focus on the bounded $^1\Sigma_g^+$ and $A^3\Sigma_u^+$ states. Fig. 2(a) plots the potential energy curve evaluated by GCGM and QUAMBO-based CI. The GCGM method produces energy in reasonable agreement with FCI for the ground state $^1\Sigma_g^+$. For the excited state $A^3\Sigma_u^+$, however, GCGM yields the wrong solution at dissociation if the RHF wave function is used as the initial trial wave function $|\Psi_0\rangle$ (see the dotted line in Fig. 2(a)). The reason is that the non-interacting $|\Psi_0\rangle$, from which the Gutzwiller wave function is constructed, does not contain the configurations of the correct wavefunction at dissociation.

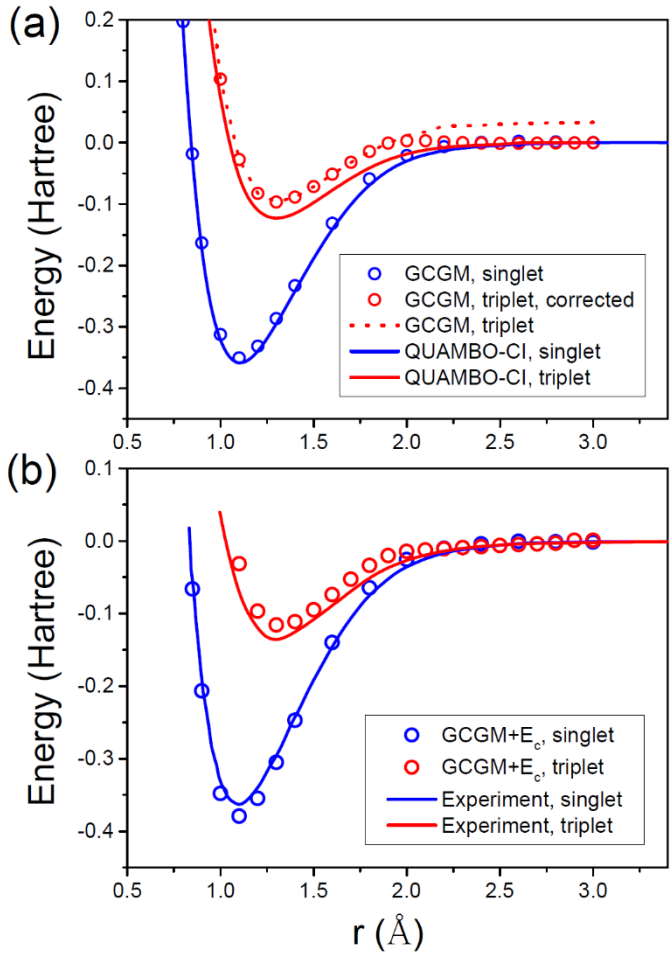

Figure 2. Potential energy curves of N_2 determined by (a) GCGM, and QUAMBO-CI, and (b) GCGM+E_c and experiment [36]. The GCGM and QUAMBO-CI calculations are based on QUAMBOs constructed from the aug-cc-pVTZ basis set.

As Ref. [29] shows, there are 2 ways to fix this problem. The 1st way is to include the atomic limit solution in the trial wave function,

$$\left|\Psi_0'\right\rangle = \left|\Psi_0\right\rangle + \lambda\left|\Psi_a\right\rangle \tag{15}$$

where $\left|\Psi_a\right\rangle$ is the atomic limit solution, and λ is the factor determing the weight of $\left|\Psi_a\right\rangle$. Then the total energy is minimized with respect to both $\{g(\Gamma_i)\}$ and λ. The 2nd way is to introduce a parameter Δ to control the dependence of $\left|\Psi_{GWF}\right\rangle$ on

$|\Psi_0\rangle$. We change the coefficient $\langle\{\Gamma_i\}|\Psi_0\rangle$ in Eq. (2) to be,

$$\langle\{\Gamma_i\}|\Psi_0\rangle = \begin{cases} \langle\{\Gamma_i\}|\Psi_0\rangle, & when \left|\langle\{\Gamma_i\}|\Psi_0\rangle\right| \geq \Delta \\ \Delta, & when \left|\langle\{\Gamma_i\}|\Psi_0\rangle\right| < \Delta \end{cases} \tag{16}$$

So the minimum of $\left|\langle\{\Gamma_i\}|\Psi_0\rangle\right|$ is set to be the adjustable Δ. $\left|\langle\{\Gamma_i\}|\Psi_0\rangle\right|$ is a number between 0 and 1 for a normalized $|\Psi_0\rangle$. By adjusting Δ, one can control the dependence of $|\Psi_{GWF}\rangle$ on $|\Psi_0\rangle$. For $\Delta = 0$, the original GCGM results are exactly reproduced. As Δ gets larger, $|\Psi_{GWF}\rangle$ gradually loses its dependence on $|\Psi_0\rangle$ and configurations which are not present in $|\Psi_0\rangle$ begin to come into play. For $\Delta = 1$, the dependence of $|\Psi_{GWF}\rangle$ on $|\Psi_0\rangle$ is fully removed. By setting Δ to be a number that is larger than 0, we allow the configurations that should be present in the atomic limit solution but are prohibited in $|\Psi_0\rangle$ to start to have an effect. Both ways can be used to obtain the correct energy at dissociation. Here we use the 2nd way to calculate the energy of the excited state $A^3\Sigma_u^+$. In principle, one needs to scan Δ ranging from 0 to 1 to get the minimal total energy. In practice, we found that it is often enough to pick up several values of Δ and get the minimal energy. Here, we use $\Delta = 0, 0.01, 1$ at each bond length and calculate the 3 corresonding energies. Then the minimum of the 3 energies is picked to plot the potential energy curve as shown in Fig. 2(a). The corrected GCGM reproduces the atomic limit energy accurately. However, GCGM overestimates the energy at the equilibrium and the region between equilibrium and dissociation. The inaccuracy may indicate the fact that the initial trial wave function $|\Psi_0\rangle$ is not a sufficiently good starting point. Fig. 2(b) plots the GCGM+E_c results in comparison with experiment [36]. With inclusion of E_c, the GCGM produces energies

in reasonable agreement with experiment, which illustrates the effectiveness of our recipe to evaluate the dynamical correlation energy.

3.3. O_2

We focus on energy calculations of the states with atomic limits being $O(^3P)+O(^3P)$. Like N_2, here we only focus on the bound states for simplicity. There are 12 bounded states, including 3 singlet and 3 triplet states. They are, sorting from lowest energy to highest energy, $X^3\Sigma_g^-$, $a^1\Delta_g$, $b^1\Sigma_g^+$, $c^1\Sigma_u^-$, $A'^3\Delta_u$, and $A^3\Sigma_u^+$. To show them clearly, we plot the potential energy curves separately for the singlet and triplet states. Fig. 3(a) and (b) plot the potential energy curves evaluated by GCGM and QUAMBO-based CI for the singlet and triplet states, respectively. For singlet states, it is enough to use RHF solution as $|\Psi_0\rangle$ to reproduce the correct energy at dissociation limit. As shown in Fig. 3(a), GCGM produces energies in reasonable agreement with QUAMBO-CI for all the 3 singlet states. For triplet states, however, the RHF solution does not contain the confugurations needed to reproduce the correct energy at dissociation. Like in the case of N_2, we use Eq. (16) to obtain the potential energy curve for the ground $X^3\Sigma_g^-$ state. Again, we use $\Delta = 0, 0.01, 1$ at each bond length and calculate the 3 corresonding energies. Then the minimum of the 3 energies is picked to plot the potential energy curve as shown in Fig. (3). For the excited triplet states $A'^3\Delta_u$ and $A^3\Sigma_u^+$, however, Eq. (16) fails to work. As all possible configurations are allowed with a minimum weight determined by Δ, these excited triplet states eventually will mix with the ground triplet state $X^3\Sigma_g^-$ after a few iterative steps towards

minimization of energy because $X^3\Sigma_g^-$ has a lower energy. In this case, Eq. (15) has to be used to correctly evaluate the energy for the excited triplet states. $|\Psi_a\rangle$, the atomic limit solution, needs to be included in the trial wave function $|\Psi_0\rangle$ with a weight determined by the factor λ. The question remains, however, as to how to determine the atomic limit solution $|\Psi_a\rangle$. First we examine why the Gutzwill wave function constructed based on the non-interactive $|\Psi_0\rangle$ fails to yield the correct energy at the dissociation limit. The triplet states have $S = 1$. If it can be described with a single Slater determinant $|\Psi_0\rangle$, S_z can only be either 1 or -1. We picked $S_z = 1$ for demonstration. When the two oxygen atoms pull away from each other towards dissociation, both atoms must have $S_z = 1/2$ from symmetry of $|\Psi_0\rangle$ and spin conservation, which is not the atomic solution (oxygen atom has $S_z = -1, 0$ or 1). So $|\Psi_0\rangle$ does not contain the correct configurations of the atomic limit solution. To fix this problem, $|\Psi_a\rangle$, the atomic limit solution, needs to be included in $|\Psi_0\rangle$. $|\Psi_a\rangle$ is set to let one oxygen atom have $S=1, S_z=1$ and the other have $S=1, S_z=0$. Then the total energy is minimized with respect to both $\{g(\Gamma_i)\}$ and λ. As shown in Fig. 3(b), GCGM yields energies in reasonable agreement with QUAMBO-CI for the 3 triplet states. Fig. 3(c) and (d) plots the GCGM+E_c results in comparison with large-basis CI [37] for singlet and triplet states, respectively. With inclusion of E_c, the GCGM generates energies in reasonable agreement with large-basis CI.

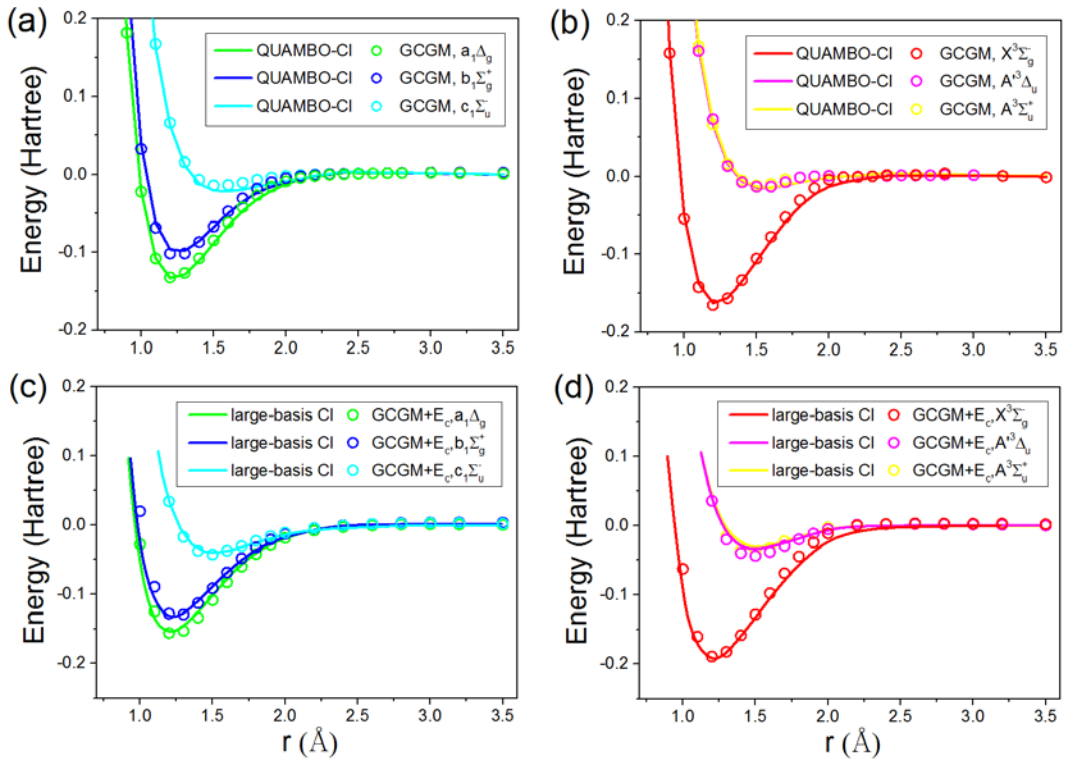

Figure 3. Potential energy curves of O_2 determined by GCGM and QUAMBO-CI for (a) singlet and (b) triplet states; GCGM+E_c and large-basis CI [37] for (c) singlet and (d) triplet states. The GCGM and QUAMBO-CI calculations are based on QUAMBOs constructed from the aug-cc-pVTZ basis set.

One may raise a question as what is the relationship between λ in Eq. (15) and Δ in Eq. (16). There is no direct relationship between the 2 adjustable parameters. λ is the factor that determines the weight of $|\Psi_a\rangle$, the atomic limit solution that needs to be included in $|\Psi_0\rangle$. Δ is the parameter that determines the minimum weight of each configuration when all configurations are to be included in $|\Psi_0\rangle$. One may also ask which one of Eq. (15) and (16) ought to be used to modify $|\Psi_0\rangle$ if $|\Psi_0\rangle$ does not include all necessary configurations. If we know what configurations should be included, we can include them in the trial wave function $|\Psi_0\rangle$, like we did for the

excited triplet states $A'^3\Delta_u$ and $A^3\Sigma_u^+$ of O_2 in Eq. (15). If we do not know what are the relevant configurations, we can use Eq. (16) to include all configurations that are not in $|\Psi_0\rangle$ by giving them a minimum weight that is determined by the adjustable parameter Δ. Nevertheless, this method may fail for some excited states. As all configurations are included, the excited states may mix with the ground state which has lower energy towards minimization of energy. In this case, we have to decide what configurations should be included and use Eq. (15) to modify $|\Psi_0\rangle$. It is still an open question as to how to find the correct configurations for complex systems.

4. CONCLUSION

Gutzwiller wavefunctions (GWF) have been widely used in describing strongly correlated systems. Methods based on the GWF can be very computationally efficient. However, the GA is a major source of inaccuracy. We recently proposed a method under the GWF framework, namely GCGM, to go beyond this inter-site decoupling approximation and boost the accuracy for energy calculation of correlated electron systems. Presently, we benchmark our GCGM method of diatomic systems, or more specifically, the H_2, N_2 and O_2. Our method provides energies for both non-magnetic and magnetic states in reasonable agreement with QUAMBO-CI, experimental measurements or large-basis CI, illustrating the power and efficiency of our approach for description of excited states, and the flexibility in the selection of initial trial wave function.

ACKNOWLEDGMENTS

This work was supported by the U.S. Department of Energy (DOE), Office of Science, Basic Energy Sciences, Materials Science and Engineering Division, including the computer time support from the National Energy Research Scientific Computing Center (NERSC) in Berkeley, CA. The research was performed at Ames Laboratory, which is operated for the U.S. DOE by Iowa State University under Contract No. DEAC02-07CH11358.

DISCLOSURE STATEMENT

No potential conflict of interest was reported by the authors.

REFERENCES

[1] P. Hohenberg and W. Kohn, Phys. Rev. **136**, B864−B871 (1964)

[2] W. Kohn and L. Sham, J. Phys. Rev. **140**, A1133−A1138 (1965)

[3] B. O. Roos, R. Lindh, P. Å. Malmqvist, V. Veryazov and P. O. Widmark, *Multiconfigurational Quantum Chemistry* (John Wiley & Sons, 2016)

[4] B. O. Roos, P. R. Taylor and P. E. M. Siegbahn, Chem. Phys. **48**, 157−173 (1980)

[5] J. Olsen, B. O. Roos, P. Jorgensen and H. J. A. Jensen, J. Chem. Phys. **89**, 2185−2192 (1988)

[6] P. A. Malmqvist, A. Rendell and B. O. Roos, J. Phys. Chem. **94**, 5477−5482 (1990)

[7] S. R. White, Phys. Rev. Lett. **69**, 2863−2866 (1992)

[8] U. Schollwöck, *Ann. Phys.* **326**, 96−192 (2011)

[9] S. R. White and A. E. Feiguin, Phys. Rev. Lett. **93**, 076401 (2004)

[10] H. Zheng and L. K. Wagner, Phys. Rev. Lett. **114**, 176401 (2015)

[11] F. Ma, W. Purwanto, S. Zhang and H. Krakauer, Phys. Rev. Lett. **114**, 226401 (2015)

[12] N. Devaux, M. Casula, F. Decremps and S. Sorella, Phys. Rev. B **91**, 081101 (2015)

[13] V. I. Anisimov, J. Zaanen and O. K. Andersen, Phys. Rev. B **44**, 943−954 (1991)

[14] V. I. Anisimov, F. Aryasetiawan and I. Lichtenstein, J. Phys.:Condens. Matter **9**, 767−808 (1997)

[15] A. Georges, G. Kotliar, W. Krauth and M. J. Rozenberg, Rev. Mod. Phys. **68**, 13−125 (1996)

[16] S. Y. Savrasov, G. Kotliar and E. Abrahams, Nature **410**, 793−795 (2001)

[17] K. M. Ho, J. Schmalian and C. Z. Wang, Phys. Rev. B **77**, 073101 (2008)

[18] Y. X. Yao, C. Z. Wang and K. M. Ho, Phys. Rev. B **83**, 245139 (2011)

[19] X. Y. Deng, L. Wang, X. Dai and Z. Fang, Phys. Rev. B **79**, 075114 (2009)

[20] N. Lanatà, H. U. R. Strand, X. Dai and B. Hellsing, Phys. Rev. B **85**, 035133 (2012)

[21] M. C. Gutzwiller, Phys. Rev. Lett. **10**, 159-162 (1963)

[22] M. C. Gutzwiller, Phys. Rev. **134**, A923 (1964)

[23] M. C. Gutzwiller, Phys. Rev. **137**, A1726 (1965)

[24] W. F. Brinkman and T. M. Rice, Phys. Rev. B **2**, 4302-4304 (1970)

[25] Y. X. Yao, J. Liu, C. Z. Wang and K. M. Ho, Phys. Rev. B **89**, 045131 (2014)

[26] Y. X. Yao, J. Liu, C. Liu, W. C. Lu, C. Z. Wang and K. M. Ho, Sci. Rep. **5**, 13478 (2015)

[27] C. Liu, J. Liu, Y. X. Yao, P. Wu, C. Z. Wang and K. M. Ho, J. Chem. Theory Comput. **12**, 4806-4811 (2016)

[28] X. Zhao, J. Liu, Y. X. Yao, C. Z. Wang and K. M. Ho, Phys. Rev. B **97**, 075142 (2018).

[29] Z. Ye, Y. X. Yao, X. Zhao, C. Z. Wang and K. M. Ho, J. Phys. Condens. Matter **31** 335601 (2019).

[30] G. C. Wick, Phys. Rev. **80**, 268-272 (1950)

[31] W. C. Lu, C. Z. Wang, M. W. Schmidt, L. Bytautas, K. M. Ho and K. J. Ruedenberg, J. Chem. Phys. **120**, 2629-2637 (2004)

[32] T. H. Dunning, J. Chem. Phys. **90**, 1007 (1989)

[33] Q. Sun *et al*. The Python-based Simulations of Chemistry Framework (PySCF). preprint, available at arXiv, https://arxiv.org/abs/1701.08223v2 (2007)

[34] T. E. Sharp, Atomic Data **2**, 119-169 (1971)

[35] C. Stemmle, B. Paulus and Ö. Legeza, Phys. Rev. A **97**, 022505 (2018)

[36] F. R. Gilmore, J. Quant. Spectrosc. Radiat. Transfer. **5**, 369-390 (1965)

[37] Z. Farooq, D. A. Chestakov, B. Yan, G. C. Groenenboom, W. J. Zande and D. H. Parker, Phys. Chem. Chem. Phys. **16**, 3305-3316 (2014)

Figure 1. Potential energy curves of H_2 determined by (a) GCGM, QUAMBO-CI and experiment [34], and (b) GCGM+E_c and experiment. The GCGM and QUAMBO-CI calculations are based on QUAMBOs constructed from the aug-cc-pVTZ basis set.

Figure 2. Potential energy curves of N2 determined by (a) GCGM, and QUAMBO-CI, and (b) GCGM+ E_c and experiment [36]. The GCGM and QUAMBO-CI calculations are based on QUAMBOs constructed from the aug-cc-pVTZ basis set.

Figure 3. Potential energy curves of O_2 determined by GCGM and QUAMBO-CI for (a) singlet and (b) triplet states; GCGM+E_c and large-basis CI [37] for (c) singlet and (d) triplet states. The GCGM and QUAMBO-CI calculations are based on QUAMBOs constructed from the aug-cc-pVTZ basis set.